Chelate-Size Effects on the Structures, Chemical Behavior, Properties, and Catalytic Activity of the New Palladium(II)−Allyl Complexes [Pd(η^3-1-R^1-C_3H_4){FcCH=N-CH_2-$(CH_2)_n$-NMe_2}][PF_6] {Fc = (η^5-C_5H_5)Fe(η^5-C_5H_4), n = 2 or 1, and R^1 = H or Ph}

Sonia Pérez,[†] Concepción López,*[,†] Ramon Bosque,[†] Xavier Solans,[‡] Mercè Font-Bardía,[‡] Anna Roig,[§] Elies Molins,[§] Piet W. N. M. van Leeuwen,[⊥,△] Gino P. F. van Strijdonck,[⊥] and Zoraida Freixa[⊥,△]

Departament de Química Inorgànica, Facultat de Química, Universitat de Barcelona, Martí i Franquès 1-11, 08028-Barcelona, Spain, Departament de Cristal·lografia, Mineralogia i Dipòsits Minerals, Facultat de Geologia, Universitat de Barcelona, Martí i Franquès s/n, 08028-Barcelona, Spain, Institut de Ciència de Materials de Barcelona (ICMAB-CSIC), Campus de la Universitat Autònoma de Barcelona, 08193-Bellaterra, Spain, Van't Hoff Institute for Molecular Sciences, University of Amsterdam, Nieuwe Achtergracht 166, 1018-WV Amsterdam, The Netherlands, and Institute of Chemical Research of Catalonia (ICIQ), Avenida Països Catalans, 16, 43007-Tarragona, Spain

Received December 13, 2007

The synthesis, X-ray crystal structures, and the study of the solution behavior of the palladium(II) allyl complexes [Pd(η^3-1R^1-C_3H_4){FcCH=N-CH_2-$(CH_2)_n$-NMe_2}][PF_6] {with Fc = (η^5-C_5H_5)Fe(η^5-C_5H_4), R^1 = H, and n = 2 (**4**) or 1 (**5**) or R^1 = Ph and n = 2 (**6**) or 1 (**7**)} are described. The structural studies of **4**, **5**, **6**, and **7** showed that the allyl ligands were bound to palladium(II) in an η^3-fashion and the ferrocenyl-Schiff bases behaved as neutral (N,N′) bidentate ligands. As observed for other Pd complexes of ligands **1** and **2**, the imine conformation of the ligand in the complex strongly depends on the length of the hydrocarbon chain between the two nitrogen donors: compounds **4** and **6** exhibited an *anti*-(*E*) conformation, whereas the *syn*-(*Z*) form is observed in **5** and **7**. ^{57}Fe-Mössbauer spectra (in the solid state) and electrochemical studies based on cyclic voltammetry of **4**, **5**, **6**, and **7** are reported. These studies reveal that the proclivity of the iron(II) toward oxidation is affected by the nature of the substituent R^1 of the allyl group {H (in **4** and **5**) or Ph (in **6** and **7**)}. Compounds **4** and **5** have been tested in the palladium(II) allylic alkylation of (*E*)-3-phenyl-2-propenyl (cinnamyl) acetate using sodium diethyl 2-methylmalonate as the nucleophile. In all cases the formation of the *trans*-(*E*) isomer of the linear product (**9**) was strongly favored versus that of the branched derivative (**10**). The stoichiometric reactions of the palladium(II) allyl intermediates [Pd(η^3-1-Ph-C_3H_4){FcCH=N-CH_2-$(CH_2)_n$-NMe_2}][PF_6] {with n = 2 (**6**) or 1 (**7**)} with the nucleophile have been studied. Density functional theory (DFT) calculations of these systems have allowed us to rationalize the structural differences as well as the regioselectivity of the catalytic and stoichiometric reactions.

Introduction

The design and development of new ligands and their transition metal complexes with applications in homogeneous catalysis is one of the actual challenges of organometallic chemistry.[1] Among the variety of catalytic reactions studied so far, those involving the formation of C−C bonds are especially attractive,[2−4] palladium(II)-catalyzed allylic alkylation being one of the most relevant processes due to its potential utility in organic synthesis.[3,4] In this reaction, the catalytic precursor is a palladium(II) complex containing an (η^3-C_3H_5) group and either one bidentate or two monodentate ligands.

One of the most widely studied catalytic allylic alkylations is that of (*E*)-3-phenyl-2-propenyl (cinnamyl) acetate or chloride with soft nucleophiles, such as sodium diethyl 2-methylmalonate. According to the mechanism accepted for this process,[4] the palladium−allyl complex formed after the oxidative addition (Scheme 1, step a) is the key intermediate of the reaction. Frequently, this intermediate isomerizes in solution, giving new species that may interchange in solution and undergo nucleophilic attack at different positions and at different rates. Consequently, four different products could be formed: the *trans*-(*E*) and *cis*-(*Z*) isomers of the achiral linear product and

* Corresponding author. E-mail: conchi.lopez@qi.ub.es. Tel: (34) 93-403-91-34. Fax: (34)-93-490-77-25.

[†] Departament de Química Inorgànica, Universitat de Barcelona.

[‡] Departament de Cristal·lografia, Mineralogia i Dipòsits Minerals, Universitat de Barcelona.

[§] Institut de Ciència de Materials de Barcelona (ICMAB-CSIC).

[⊥] University of Amsterdam.

[△] Institute of Chemical Research of Catalonia.

(1) For a general overview of the recent advances in this field, see for instance the special issue devoted to "New organometallics compounds for applications in homogeneous catalysis" published in *J. Organomet. Chem.* **2006**, *691*.

(2) (a) Jacobsen, E. N., Pfaltz, A., Yamamoto, H., Eds. *Comprehensive Asymmetric Catalysis*; Springer: Berlin (Germany), 1999; Vols. *I*−*III*. (b) van Leeuwen, P. W. N. M. *Homogeneous Catalysis. Understanding the Art*; Kluwer Academic Publishers: Dordrecht (The Netherlands), 2004.

(3) Ojima, I. *Catalysis Asymmetric Synthesis*, 2nd ed.; Wiley-VCH: New York, 2000.

(4) (a) Trost, B. M. *J. Org. Chem.* **2004**, *69*, 5813–5837. (b) Colacot, T. J. *Chem. Rev.* **2003**, *103*, 3101–3118. (c) Helmchen, G; Ernst, M.; Paradies, G. *Pure Appl. Chem.* **2004**, *76*, 495–505.

10.1021/om7012452 CCC: $40.75
Publication on Web 08/07/2008

Scheme 1. Main Steps of the Catalytic Allylic Alkylation of Substrates Ph-CH=CH-CH_2(LG) (LG = AcO or Cl; Nu^- represents the nucleophile)

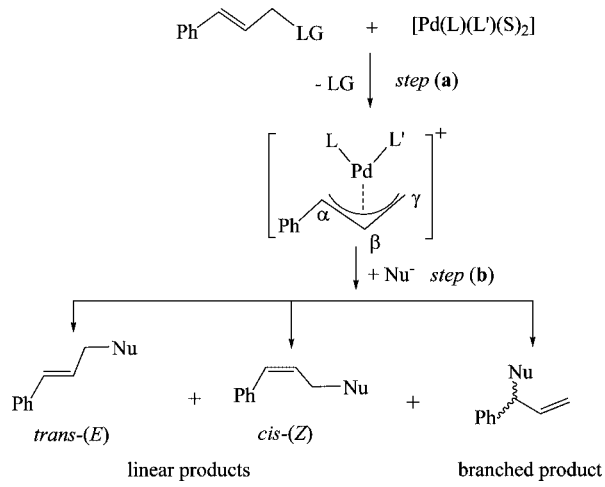

the two enantiomers of the chiral branched derivative (Scheme 1, step b). In these cases enantioselectivity can be envisaged only when regioselectivity is under control, and to this end understanding the factors that govern regioselectivity becomes crucial.[5]

On the other hand, and despite the interest in ferrocene derivatives in catalytic processes[6,7] including enantioselective allylic alkylation,[8] the effect of the electronic properties of two different donor atoms of the ligand on the regioselectivity of the process has not been studied in detail,[9−11] and studies using ferrocenyl ligands containing two nitrogen atoms with different electronic properties have not been carried out so far. Synthesis of ferrocenyl derivatives is well developed, and ferrocene is a bulky group exerting a directing influence on the structures being formed. Thus, we set out to prepare and characterize the palladium(II) allyl complexes $[Pd(\eta^3\text{-}1\text{-}R^1\text{-}C_3H_4)\{FcCH{=}N\text{-}CH_2\text{-}(CH_2)_n\text{-}NMe_2\}]^+$ (n = 2 or 1 and R = H or Ph) derived from $[FcCH{=}N\text{-}CH_2\text{-}(CH_2)_n\text{-}NMe_2]$ {n = 2 (**1**) or 1 (**2**)}[12,13] (Figure 1)} and to study their properties.

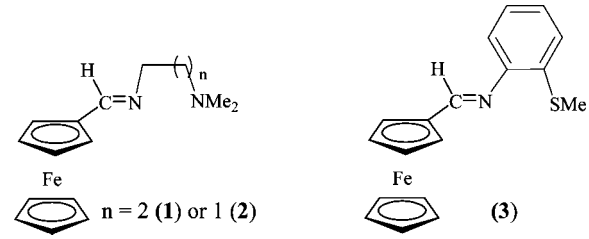

Figure 1. Schematic view of ligands under study [FcCH=N-CH_2-$(CH_2)_n$-NMe_2] {with n = 2 (**1**) or 1 (**2**)} and of the Ferrocenyl Schiff Base [FcCH=N-(C_6H_4-2SMe)] (**3**) Reported Previously.

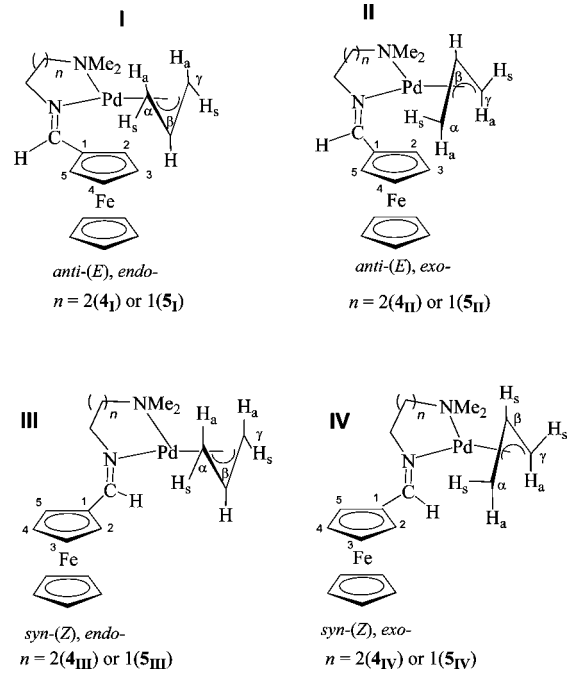

Figure 2. Simplified view of the main isomeric forms that could be expected for the cations of compounds $[Pd(\eta^3\text{-}C_3H_5)\{FcCH{=}N\text{-}CH_2\text{-}(CH_2)_n\text{-}NMe_2\}][PF_6]$ {n = 2 (**4**) or 1 (**5**)}.

Results and Discussion

Synthesis and Characterization. Compounds $[Pd(\eta^3\text{-}1R^1\text{-}C_3H_4)\{FcCH{=}N\text{-}CH_2\text{-}(CH_2)_n\text{-}NMe_2\}][PF_6]$ {R^1 = H and n = 2 (**4**) or 1 (**5**) or R^1 = Ph and n = 2 (**6**) or 1 (**7**)} were prepared in acetone by treatment of the corresponding palladium(II) dimer $[Pd(\eta^3\text{-}1R^1\text{-}C_3H_4)(\mu\text{-}Cl)]_2$ (R^1 = H or Ph)[14] with the proper ligand $[FcCH{=}N\text{-}CH_2\text{-}(CH_2)_n\text{-}NMe_2]$ {n = 2 (**1**) or 1 (**2**)}[12,13] {in a molar ratio (**1** or **2**):Pd(II) = 1} and in the presence of an excess (20%) of $K[PF_6]$. The new products are stable, orange (for **4** and **5**) or light red

(5) (a) Oosterom, G. E.; van Haaren, R. J.; Reek, J. N. H.; Kamer, P. C. J.; van Leeuwen, P. W. N. M. *Chem. Commun.* **1999**, 1119–1120. (b) van Haaren, R. J.; Goubits, K.; Fraanje, J.; van Strijdonck, G. P. F.; Oevering, H.; Coussens, B.; Reek, J. N. H.; Kamer, P. C. J.; van Leeuwen, P. W. N. M. *Inorg. Chem.* **2001**, *40*, 3363–3372.

(6) Togni, A., Hayashi, T., Eds. *Ferrocenes. Homogeneous Catalysis. Organic Synthesis and Material Science*; VCH: Weinheim (Germany), 1995.

(7) For recent contributions on the utility of transition metal complexes containing ferrocenyl ligands in homogeneous catalysis see for instance: (a) Anderson, C. E.; Donde, Y.; Douglas, C. J.; Overman, L. E. *J. Org. Chem.* **2005**, *70*, 648–657. (b) Moyano, A.; Rosol, M.; Moreno, R. M.; López, C.; Maestro, M. A. *Angew. Chem., Int. Ed.* **2005**, *44*, 1865–1869. (c) He, P.; Lu, Y.; Dong, C.-G.; Hu, Q.-S. *Org. Lett.* **2007**, *9*, 343–346. (d) Teo, S.; Weng, Z.; Hor, T. S. A. *Organometallics* **2006**, *25*, 1199–1205. (e) Gómez Arrayás, R.; Adrio, J.; Carretero, J. C. *Angew. Chem., Int. Ed* **2006**, *45*, 7674–7715.

(8) (a) García Manchero, O.; Priego, J.; Cabrera, S.; Gómez Arrayás, R.; Llamas, T.; Carretero, J. C. *J. Org. Chem.* **2003**, *68*, 3679–3686. (b) Sturm, T.; Abad, B.; Weissensteiner, W.; Mereiter, K.; Manzano, B. R.; Jalón, F. A. *J. Mol. Catal. A.* **2006**, *255*, 209–219. (c) Raghunath, M.; Gao, W.; Zhang, X. *Tetrahedron: Asymmetry* **2005**, *16*, 3676–3681. (d) Mateus, N.; Routaboul, L.; Daran, J. C.; Manoury, E. *J. Organomet. Chem.* **2006**, *691*, 2297–3310. (e) Routaboul, L.; Vincendeau, S.; Daran, J. C.; Manoury, E. *Tetrahedron: Asymmetry* **2005**, *16*, 2685–2690. (f) Anderson, J. C.; Osborne, J. *Tetrahedron: Asymmetry* **2005**, *16*, 931–934. (g) Lam, F. L.; Au-Yeung, T. T. L.; Cheung, H. Y.; Kok, S. H. L.; Lam, W. S.; Wong, K. Y.; Chan, A. C. S. *Tetrahedron: Aymmetry* **2006**, *17*, 497–499. (h) You, S. L.; Hou, X. K.; Dai, L. X.; Yu, H. Y.; Xia, W. *J. Org. Chem.* **2002**, *67*, 4684–4695.

(9) Zheng, W. H.; Sun, N.; Hou, X. L. *Org. Lett.* **2005**, *7*, 5151–5154, and references therein.

(10) Co, T. T.; Paek, S. W.; Shim, S. C.; Cho, C. S.; Kim, T. J.; Choi, D. W.; Kang, S. O.; Jeong, J. H. *Organometallics* **2003**, *22*, 1475–1482.

(11) López, C.; Pérez, S.; Solans, X.; Font-Bardía, M.; Roig, A.; Molins, E.; van Leeuwen, P. W. N. M.; van Strijdonck, G. P. F. *Organometallics* **2007**, *26*, 571–576.

(12) López, C.; Caubet, A.; Pérez, S.; Solans, X.; Font-Bardía, M. *J. Organomet. Chem.* **2002**, *651*, 105–113.

(13) (a) Caubet, A.; López, C.; Bosque, R.; Solans, X.; Font-Bardía, M. *J. Organomet. Chem.* **1999**, *577*, 292–304. (b) Bosque, R.; Caubet, A.; López, C.; Espinosa, E.; Molins, E. *J. Organomet. Chem.* **1997**, *544*, 233–241.

(14) (a) Szafran, Z.; Pike, P. E.; Singh, M. M., *Microscale Inorganic Chemistry. A Comprehensive Laboratory Experience*; John Wiley & Sons: New York, 1991. (b) Auburn, P. R.; Mackenzie, P. B.; Bosnich, B. *J. Am. Chem. Soc.* **1985**, *107*, 2033–2046.

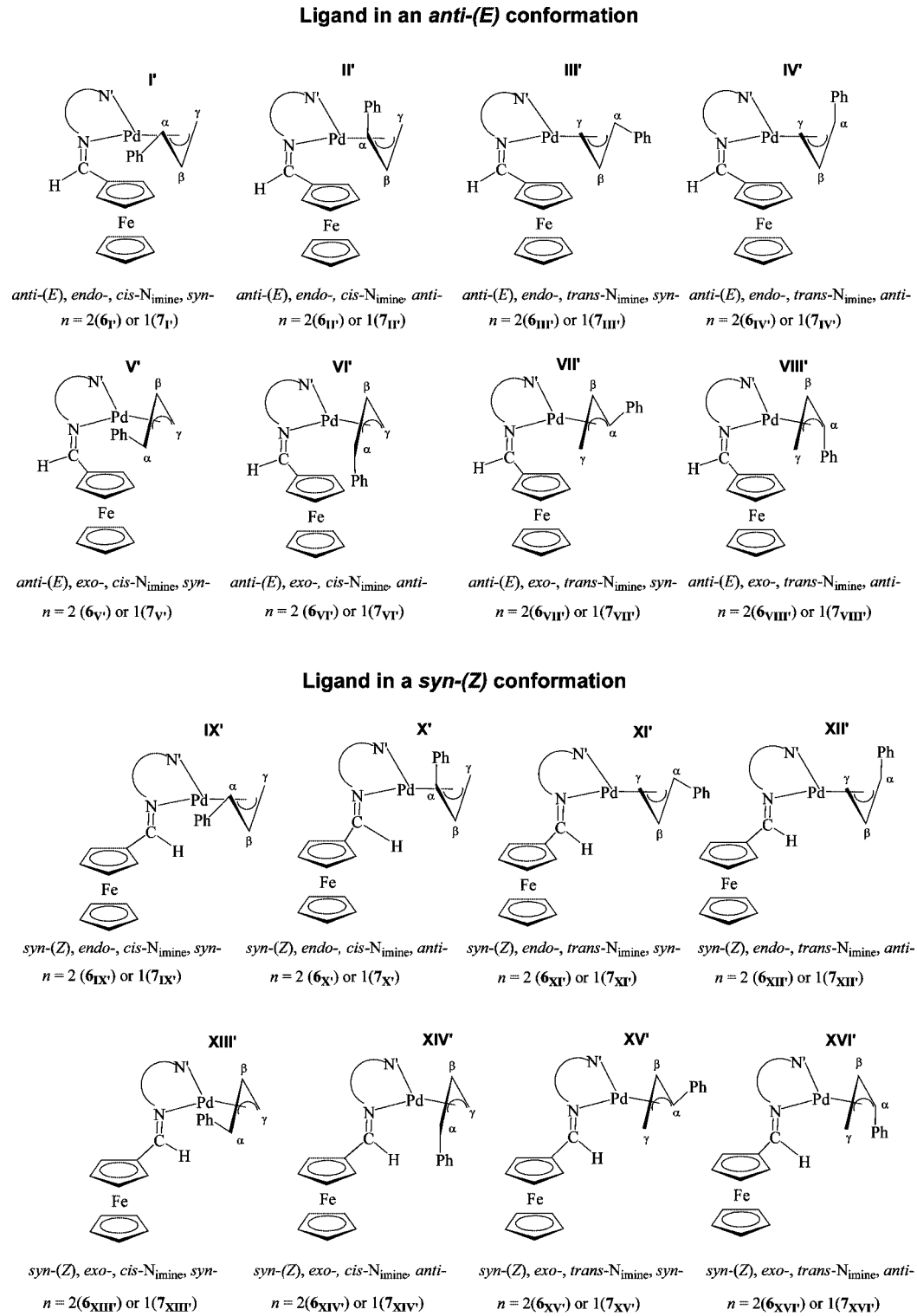

Figure 3. Simplified view of the main isomeric forms expected for cations of compounds $[Pd(\eta^3\text{-}1\text{-}Ph\text{-}C_3H_4)\{FcCH{=}N\text{-}CH_2\text{-}(CH_2)_n\text{-}NMe_2\}][PF_6]$ {$n = 2$ (**6**) or 1 (**7**)}. The Schiff base adopts the *anti*-(*E*) conformation in **I′**−**VIII′** and the *syn*-(*Z*) form in **IX′**−**XVI′**. (Most hydrogen atoms have been omitted for clarity).

(for **6** and **7**) solids at room temperature. They are insoluble in *n*-hexane and diethyl ether but exhibit high solubility in acetone, acetonitrile, chloroform, and dichloromethane. Unfortunately, compounds **4** and **5** slowly degrade in the latter solvent, giving ferrocenecarboxaldehyde (probably formed by hydrolysis of the ligand).[15] This precluded carrying out NMR spectroscopic studies of **4** and **5** in these solvents. The four allyl compounds **4**−**7** were characterized in the solid state by elemental analyses, mass spectrometry, infrared spectroscopy, X-ray diffraction, and ^{57}Fe-Mössbauer spectroscopy. Solution studies based on one- [^{1}H and ^{13}C{^{1}H}] and two-dimensional [(^{1}H−^{1}H) COSY and NOESY and heteronuclear (^{1}H−^{13}C) correlations (HSQC and HMBC)] NMR spectra were also carried out in different solvents to characterize the compounds.

Elemental analyses of **4**−**7** were consistent with the proposed formulas, and the FAB$^+$ mass spectra showed peaks due to the cations $[Pd(\eta^3\text{-}1\text{-}R^1\text{-}C_3H_4)\{FcCH{=}N\text{-}CH_2\text{-}(CH_2)_n\text{-}NMe_2\}]^+$ (at

m/*z* = 445, 431, 521, and 507 for **4**, **5**, **6**, and **7**, respectively). One of the most outstanding features observed in the IR spectra of **4**−**7** was the presence of a sharp band at ca. 1610−1635 cm^{-1}, due to the stretching of the >C═N− group.[11,16] This band appears at lower frequencies than that of the free ligands (**1** or **2**).[12,13] This is consistent with the binding of the imine nitrogen to the palladium(II) ion.[15−17] The typical bands due to the $[PF_6]^-$ anion[18] were also identified in the IR spectra of **4**−**7**.

Due to the characteristics of the ligands bound to the palladium(II) in **4** and **5**, the formation of a wide variety of different isomeric forms could be expected (Figure 2). These may differ in (a) the conformation of the imine {*anti*-(*E*) or *syn*-(*Z*)} and/or (b) the relative orientation between the "Fe(η^5-C_5H_5)" moiety and the central C−H bond of the coordinated allyl group. These two fragments may be located on the same side of the coordination plane of the palladium(II) (*endo* type) (Figure 2, **I** and **III**) or on opposite sides (*exo* type) (Figure 2, **II** and **IV**). In addition to the isomeric forms depicted in Figure 2 the nonplanar six- (in **4**) or five- (in **5**) membered chelate rings, formed by the coordination of the two heteroatoms to the palladium(II), may also exhibit different conformations.[19] Finally, if the rotation around the C_{ipso}−C_{imine} bond of the ferrocenyl moiety is hindered, then rotameric species could be generated, especially at low temperatures.

As a consequence of the asymmetry of the chelating (N,N′) ligands and that of the 1-Ph-C_3H_4 group, compounds **6** and **7** could form an even larger number of isomeric species (Figure 3) than their analogues **4** and **5** (Figure 2). In addition to the differences arising from the conformation of the ligand {*anti*-(*E*) or *syn*-(*Z*) (Figure 3, **I′**−**VIII′** and **IX′**−**XVI′**, respectively} and the relative arrangement of the allyl group versus the "Fe(η^5-C_5H_5)" fragment (*endo* or *exo*), in the isomers of **6** and **7** (a) the substituted carbon of the allyl group (hereafter referred to as C^{α}) could be in a *cis*- or *trans*-arrangement versus the imine nitrogen of the Schiff base and (b) the phenyl group and the central hydrogen of the 1-Ph-C_3H_4 unit could be in a *syn*- or *anti*-orientation (Figure 3).

Description of the Crystal Structures. The crystal structure of [Pd(η^3-C_3H_5){FcCH═N-CH_2-$(CH_2)_2$-NMe_2}][PF_6] (**4**) consists of equimolar amounts of [Pd(η^3-C_3H_5){FcCH═N-CH_2-$(CH_2)_2$-NMe_2}]$^+$ cations and $[PF_6]^-$ anions. In the cations (Figure 4) the palladium(II) atom is bound to the C_3H_5 moiety in a η^3-fashion and to the two nitrogen atoms {N(1) and N(2)} of the ferrocenyl ligand, resulting in a slightly distorted square-planar environment.

The differences observed in Pd−N bond lengths {Pd−N(1), 2.083(6) Å; Pd−N(2), 2.170(7) Å} are similar to those found in *cis*-[Pd{FcCH═N-CH_2-$(CH_2)_2$-NMe_2}Cl_2] previously described.[12] The >C═N− bond length [1.286(6) Å] agrees with the values found for most of the ferrocenylaldimines[20,21] and their transition metal complexes.[11−13,17,20,22,23] The value of the torsion angle C(10)−C(11)−N(1)−C(12) is 176.8(5)°, indicating that the "-$(CH_2)_3$-NMe_2" fragment and the "Fc" moiety are in a *trans*-arrangement {*anti*-(*E*) conformation of the ligand}.

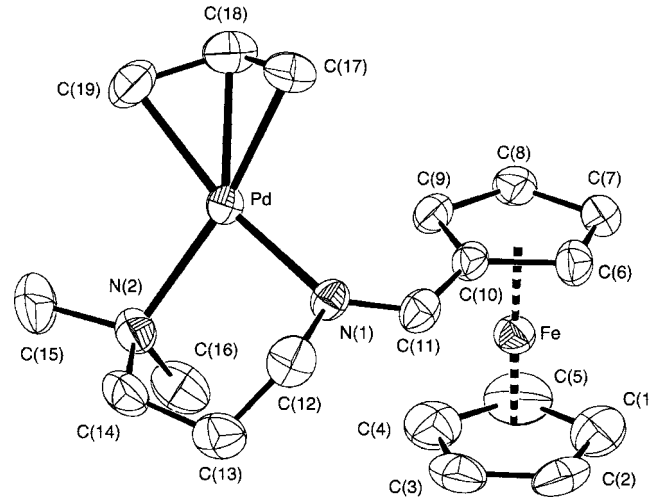

Figure 4. ORTEP plot of the cationic array of [Pd(η^3-C_3H_5){FcCH═N-CH_2-$(CH_2)_2$-NMe_2}][PF_6] (**4**). Hydrogen atoms have been omitted for clarity. Selected bond lengths (in Å) and angles (in deg): Pd−N(1), 2.083(6); Pd−N(2), 2.170(7); Pd−C(17), 2.112(8); Pd−C(18), 2.145(10); Pd−C(19), 2.114(9); C(10)−C(11), 1.470(1); N(1)−C(11), 1.280(10); N(1)−C(12), 1.462(11); C(12)−C(13), 1.524(14); C(13)−C(14), 1.490(15); C(14)−N(2), 1.501(12); N(2)−C(15), 1.492(11); C(17)−C(18), 1.374(15); C(18)−C(19), 1.412(14); N(1)−Pd−N(2), 88.4(3); N(1)−Pd−C(17), 97.8(4); N(1)−Pd−C(19), 165.8(4); C(17)−Pd−C(19), 69.1(4); C(17)−Pd-C(18), 37.6(4); C(19)−Pd−C(18), 38.7(4); C(10)−C(11)−N(1), 125.7(7); C(11)−N(1)−C(12), 116.1(5); and C(17)−C(18)−C(19), 118.7(10).

The allyl group binds to palladium(II) in a η^3-fashion, and the plane defined by the atoms C(17), C(18), and C(19) forms an angle of 118.4(3)° with the coordination plane of palladium(II). The C−C bond lengths of the allyl group and the bond angle C(17)−C(18)−C(19) agree with data reported for other palladium(II) complexes possessing an η^3-C_3H_5 ligand.[10,20,24] The central carbon atom of the allyl group {C(18)} and the "Fe(η^5-C_5H_5)" moiety are on the same side of the coordination plane of the palladium(II) (*endo*-type conformation). Thus, the arrangement of groups found in this cation corresponds to the {*anti*-(*E*), *endo*} isomer (**4$_I$** in Figure 2).

The six-membered ring formed by the binding of the two nitrogen atoms to the palladium has a chair conformation, where the C(13) atom and the palladium deviate −0.681 and 1.167 Å, respectively, from the main plane defined by the set of atoms N(1), C(12), C(14), and N(2).

The X-ray crystal structure of [Pd(η^3-C_3H_5){FcCH═N-CH_2-CH_2-NMe_2}][PF_6] (**5**) is formed by two different units of cations

(15) The partial hydrolysis of ferrocenylaldimines has been reported in the following articles: (a) López, C.; Caubet, A.; Pérez, S.; Solans, X.; Font-Bardía, M. *Chem. Commun.* **2004**, *54*, 0–541. (b) López, C.; Caubet, A.; Pérez, S.; Solans, X.; Font-Bardía, M.; Molins, E. *Eur. J. Inorg. Chem.* **2006**, *397*, 4–3984. (c) Pérez, S.; López, C.; Caubet, A.; Solans, X.; Font-Bardía, M. *New J. Chem.* **2003**, *27*, 975–982.

(16) (a) López, C.; Sales, J; Solans, X.; Zquiak, R. *J. Chem. Soc., Dalton Trans.* **1992**, 1637–1646. (b) Bosque, R.; López, C.; Sales, J.; Solans, X.; Font-Bardía, M. *J. Chem. Soc., Dalton Trans.* **1994**, 735–737.

(17) (a) Wu, Y.; Huo, S.; Gong, J.; Cui, X.; Ding, L.; Ding, K.; Du, C.; Song, M. *J. Organomet. Chem.* **2001**, *637*−*639*, 27–46. (b) López, C.; Caubet, A.; Bosque, R.; Solans, X.; Font-Bardía, M. *J. Organomet. Chem.* **2002**, *645*, 146–151.

(18) Nakamoto, K. *IR and Raman Spectra of Inorganic and Coordination Compounds*, 5th ed.; John Wiley & Sons: New York, 1997.

(19) Harrowfield, J. MacB.; Wild, B. S. In *Comprehensive Coordination Chemistry. The Synthesis, Reactions, Properties and Applications of Coordination Compounds*; Wilkinson, G., Gillard, R. D., Cleverty, J. A. Mc., Eds.; Pergamon Press: Exeter (UK), 1987; Vol. 1, Chapter 5, p 196.

(20) Allen, F. H. *Acta Crystallogr.* **2002**, *B58*, 380–388.

(21) López, C.; Bosque, R.; Solans, X.; Font-Bardía, M. *New J. Chem.* **1996**, *20*, 1285–1292.

(22) López, C.; Caubet, A.; Pérez, S.; Bosque, R.; Solans, X.; Font-Bardía, M. *Polyhedron* **2002**, *21*, 2361–2367.

(23) (a) López, C.; Bosque, R.; Sainz, D.; Solans, X.; Font-Bardía, M. *Organometallics* **1997**, *16*, 3261–3266. (b) López, C.; Caubet, A.; Solans, X.; Font-Bardía, M. *J. Organomet. Chem.* **2000**, *598*, 87–102.

(24) von Matt, P.; Lloyd-Jones, G. C.; Minidis, A. B. E.; Pfaltz, A.; Macko, L.; Neuburger, M.; Zehnder, M.; Rüegger, H.; Pregosin, P. S. *Helv. Chim. Acta* **1995**, *78*, 265–284.

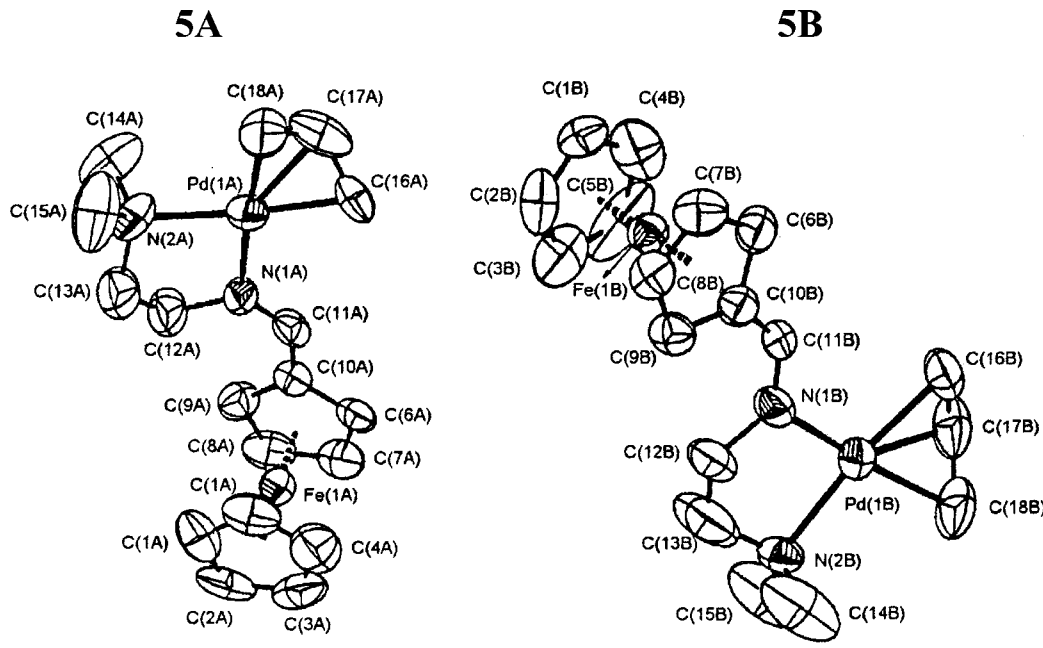

Figure 5. ORTEP plots of the two nonequivalent cations (**5A** and **5B**) of [Pd(η^3-C_3H_5){FcCH═N-CH_2-CH_2-NMe_2}][PF_6] (**5**). Hydrogen atoms have been omitted for clarity. Selected bond lengths (in Å) and angles (in deg): Pd(1A)−N(1A), 2.08(6); Pd(1B)−N(1B), 2.07(8); Pd(1A)−N(2A), 2.14(7); Pd(1B)−N(2B), 2.13(7); Pd(1A)−C(16A), 2.07(6); Pd(1B)−C(16B), 2.07(9); Pd(1A)−C(17A), 2.09(10); Pd(1B)−C(17B), 2.11(10); Pd(1A)−C(18A), 2.11(9); Pd(1B)−C(18B), 2.09(10); N(1A)−C(11A), 1.27(10); N(1B)−C(11B), 1.28(11); N(1A)−C(12A), 1.44(11); N(1B)−C(12B), 1.45(11); C(10A)−C(11A), 1.43(11); C(10B)−C(11B), 1.46(13); C(16A)−C(17A), 1.30(14); C(16B)−C(17B), 1.34(14); C(17A)−C(18A), 1.31(14); C(17B)−C(18B), 1.39(14); N(1A)−Pd(1A)−N(2A), 81(2); N(1B)−Pd(1B)−N(2B), 82(3); C(16A)−Pd(1A)−N(1A), 107(3); C(16B)−Pd(1B)−N(1B), 106(4); C(16A)−Pd(1A)−C(17A), 36(4); C(16B)−Pd(1B)−C(17B), 38(4); N(1A)−Pd(1A)−C(17A), 139(4); N(1B)−Pd(1B)−C(17B), 141(4); C(16A)−Pd(1A)−C(18A), 67(4); C(16B)−Pd(1B)−C(18B), 68(4); C(16A)−Pd(1A)−N(2A), 172(3); C(16B)−Pd(1B)−N(2B), 172(4); C(10A)−C(11A)−N(1A), 132(8); C(10B)−C(11B)−N(1B), 130(8); C(16A)−C(17A)−C(18A), 125(10); C(16B)−C(17B)−C(18B), 116(10). Cations **5A** and **5B** correspond to {*syn*-(*Z*), *exo*} and {*syn*-(*Z*), *endo*} isomers, respectively.

Table 1. Iron-57 Mössbauer Hyperfine Parameters: Isomer Shift (i.s.), Quadrupole Splitting (ΔE_q), and Full-Width at Half-Height (Γ) (in mm s^{-1}) for Compounds [Pd(η^3-1-R^1-C_3H_5){FcCH═N-CH_2-$(CH_2)_n$-NMe_2}][PF_6] {R^1 = H and n = 2 (4) or 1 (5) or R^1 = Ph and n = 2 (6) or 1 (7)}

compound	n	R^1	i.s.	ΔE_q	Γ
4	2	H	0.522(1)	2.243(2)	0.229(4)
5	1	H	0.525(1)	2.237(2)	0.224(4)
6	2	Ph	0.498(2)	2.306(2)	0.239(4)
7	1	Ph	0.489(2)	2.245(6)	0.258(8)

[Pd(η^3-C_3H_5){FcCH═N-CH_2-CH_2−NMe_2}]$^+$ (hereafter referred to as **5A** and **5B**) (Figure 5) and [PF_6]$^-$ anions.

In the two cations the Pd−N bond lengths are also greater than in the coordination complex *cis*-[Pd{FcCH═N-CH_2-(CH_2)-NMe_2}Cl_2][13a] (Table 1). The differences between the bond distances Pd−N(1) and Pd−N(2) in cations **5A** and **5B** do not clearly exceed 3σ, and a similar trend is found for the bond distances between the palladium(II) and the terminal atoms of the allyl group {C(16A) and C(18A) or C(16B) and C(18BA) in cations **5A** and **5B**, respectively}.

The main planes of the allyl moieties form angles of 113(1)° (in **5A**) and 117(1)° (in **5B**) with the coordination plane of the corresponding palladium(II). In the two cations, the five-membered rings formed by the binding of the two nitrogen atoms to the palladium atoms have envelope-like conformation in which the C(13A) (in **5A**) and C(13B) (in **5B**) deviate from the plane defined by the sets of atoms [Pd(1A), N(1A), C(12A), and N(2A)] (in **5A**) and [Pd(1B), N(1B), C(12B), and N(2B)] (in **5B**).

In contrast with the results obtained for **4**, in **5** the ligand adopts the *syn*-(*Z*) conformation in cations **5A** and **5B**, as reflected in the values of the torsion angles C(10A)−C(11A)−N(1A)−C(12A) and C(10B)−C(11B)−N(1B)−C(12B) (4.9° and 6.0°, respectively).

The main difference between cations **5A** and **5B** is the relative orientation between the central carbon atom of the allyl moiety {C(17A) and C(17B)} and the "Fe(η^5-C_5H_5)" unit of the same cation. In **5A** these two groups are located at opposite sides of the coordination plane (*exo*), while in **5B**, they are at the same side (*endo*). Thus, the structural characterization of this product reveals that cations **5A** and **5B** correspond to the {*syn*-(*Z*), *exo*} and {*syn*-(*Z*), *endo*} isomers (Figure 2, types **IV** and **III**, respectively).

The crystal structure of **6** is formed by [Pd(η^3-1-Ph-C_3H_4){FcCH═N-CH_2-$(CH_2)_2$-NMe_2}]$^+$ cations and [PF_6]$^-$ anions. As can be seen in Figure 6, the palladium(II) ion is bound to the two nitrogen atoms of the ferrocenyl Schiff base and to the (1-Ph-C_3H_4) group in a η^3-fashion. Similarly to what is observed in the X-ray structure of cation **4**, in the cation of **6**, the Pd−N(2) bond is larger than the Pd−N(1) bond. The differences detected in the Pd−C(17) and Pd−C(19) bond lengths {2.101(8) and 2.180(7) Å, respectively} suggest that the allyl moiety is asymmetrically bound to palladium, but the two C−C bond lengths of this ligand are practically identical {C(17)−C(18) = 1.385(10) Å and C(18)−C(19) = 1.384(10) Å}.

The value of the torsion angle C(10)−C(11)−N(1)−C(12) (172.2°) indicates that the ligand adopts the *anti*-(*E*) conformation. The central C−H bond of the allyl group and the unsubstituted pentagonal ring of the ferrocenyl unit are located at opposite sides of the coordination plane of the palladium (*exo*). The substituted carbon C(19) of the allyl group is in a

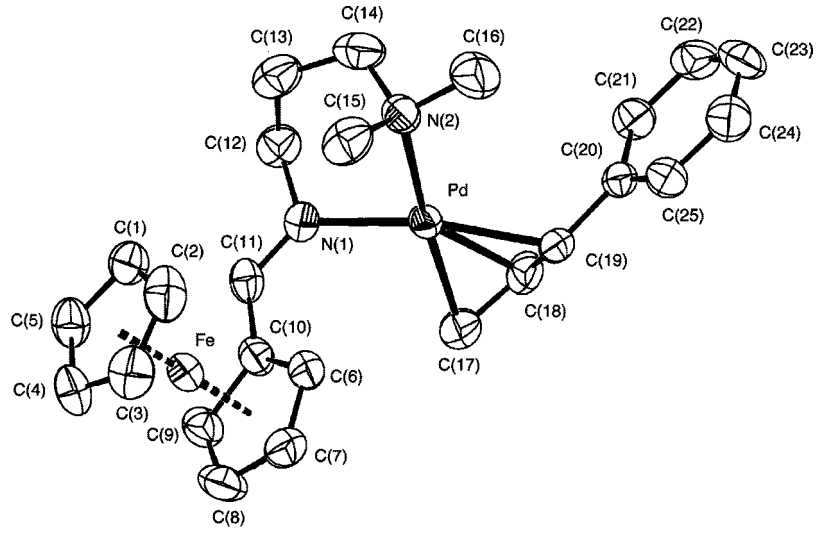

Figure 6. Molecular structure of $[Pd(\eta^3\text{-}1\text{-}Ph\text{-}C_3H_4)\{FcCH{=}N\text{-}CH_2\text{-}(CH_2)_2\text{-}NMe_2\}][PF_6]$ (**6**). The $[PF_6]^-$ anion and hydrogen atoms have been omitted for clarity. Selected bond lengths (in Å) and angles (in deg): Pd−N(1), 2.083(5); Pd−N(2), 2.160(5); Pd−C(17), 2.101(8); Pd−C(18), 2.097(7); Pd−C(19), 2.180(7); C(10)−C(11), 1.453(10); C(11)−N(1), 1.312(9); N(1)−C(12), 1.454(9); C(12)−C(13), 1.490(12); C(13)−C(14), 1.531(12); C(14)−N(2), 1.461(9); N(2)−C(15), 1.512(10); N(2)−C(16), 1.485(10); C(17)−C(18), 1.385(10); C(18)−C(19), 1.384(10); C(19)−C(20), 1.485(10); N(1)−Pd−N(2), 87.4(2); N(1)−Pd−C(17), 98.3(3); N(2)−Pd−C(19), 106.6(2); C(17)−Pd−C(19), 67.8(3); C(10)−C(11)−N(1), 125.3(6); C(11)−N(1)−C(12), 118.5(6); N(1)−C(12)−C(13), 110.2(6); C(12)−C(13)−C(14), 116.7(7); C(13)−C(14)−N(2), 116.1(6); C(14)−N(2)−C(15), 110.2(6); C(14)−N(2)−C(16), 107.5(7); C(16)−N(2)−C(15), 106.2(7); C(17)−C(18)−C(19), 119.2(7); C(18)−C(19)−C(20), 123.5(6); C(19)−C(20)−C(21), 124.3(6); C(19)−C(20)−C(25), 117.9(6).

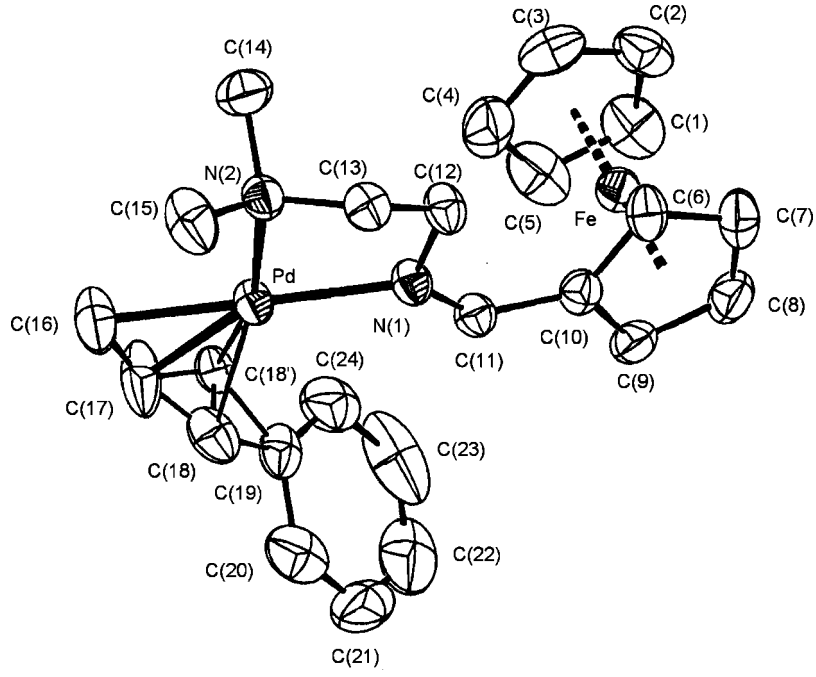

Figure 7. Molecular structure of $[Pd(\eta^3\text{-}1\text{-}Ph\text{-}C_3H_4)\{FcCH{=}N\text{-}CH_2\text{-}CH_2\text{-}NMe_2\}][PF_6]$ (**7**). The $[PF_6]^-$ anion and hydrogen atoms have been omitted for clarity. Selected bond lengths (in Å) and angles (in deg): Pd−N(1), 2.097(3); Pd−N(2), 2.130(3); Pd−C(16), 2.099(4); Pd−C(17), 2.094(5); Pd−C(18), 2.209(9); Pd−C(18′), 2.206(6); C(10)−C(11), 1.446(5); N(1)−C(11), 1.280(4); N(1)−C(12), 1.463(4); C(12)−C(13), 1.514(5); C(13)−N(2), 1.474(5); N(2)−C(14), 1.475(6); N(2)−C(15), 1.483(6); N(1)−Pd−N(2), 81.93(12); N(1)−Pd−C(16), 174.0(2); N(1)−Pd−C(17), 139.66(16); C(16)−Pd−N(2), 102.08(18); C(17)−Pd−N(2), 138.29(18); C(17)−Pd−C(18), 32.7(4); C(17)−Pd−C(18′), 34.8(2); N(1)−Pd−C(18), 109.6(2); N(1)−Pd−C(18′), 106.6(2);C(10)−C(11)−N(1), 132.0(3); C(11)−N(1)−C(12), 120.1(3); C(12)−C(13)−N(2), 109.2(3); C(13)−N(2)−C(14), 110.7(3); C(13)−N(2)−C(15), 107.8(4); C(14)−N(2)−C(15), 109.5(5).

trans-arrangement to the imine nitrogen and the phenyl ring occupies a *syn*-position in relation to the central C−H bond of the 1-Ph-C_3H_4 unit. All these findings indicate that the structure presented in Figure 6 corresponds to the {*anti*-(*E*), *exo, trans*-N_{imine}, *syn*} isomer ($\mathbf{6_{VII'}}$ in Figure 3).

The unit cell of **7** contains the heterodimetallic cations $[Pd(\eta^3\text{-}1\text{-}Ph\text{-}C_3H_4)\{FcCH{=}N\text{-}CH_2\text{-}CH_2\text{-}NMe_2\}]^+$ and $[PF_6]^-$ anions in a 1:1 molar ratio. In the cationic array (Figure 7) the palladium(II) is in a slightly distorted square-planar environment bound to the two nitrogen atoms of the chelating ligand. The Pd−N(1) and Pd−N(2) bond lengths are similar to those reported for **5**, and the two remaining coordination sites are occupied by the allyl moiety that exhibits a η^3-hapticity. In this case the imine adopts the *syn*-(*Z*)

conformation, as reflected in the value of the torsion angle C(10)−C(11)−N(1)−C(12): 1.80°.

The C−C bond distances of the allyl group are consistent with those reported for other palladium(II) complexes containing the 1-Ph-C_3H_4 group.[20] Unfortunately, the substituted carbon atom of the allyl group was found disordered, and an occupancy factor of 0.5 was assigned to the two positions {C(18) and C(18′)}. The two situations defined by the C(18) and C(18′) atoms respectively correspond to different orientations of the allyl group versus the "Fe(η^5-C_5H_5)" unit {*endo* for C(18) and *exo* for C(18′)}. The C(18) or C(18′) atoms of the allyl group are located in a *cis*-arrangement to the imine nitrogen, and this arrangement of groups is different from that found for **6**. In both cases the relative arrangement between the aryl group and the central C−H bond is *syn*. Thus, the two limit situations defined by the position of C(18) and C(18′) correspond to the {*syn*-(*Z*), *endo, cis*-N_{imine}, *syn*} and {*syn*-(*Z*), *exo, cis*-N_{imine}, *syn*} isomers (Figure 3, $\mathbf{7_{IX'}}$ and $\mathbf{7_{XIII'}}$, respectively).

For the four crystal structures described here, bond lengths and angles of the ferrocenyl unit agree with the values reported for most of the ferrocene derivatives,[12,15,20,21,25] the two pentagonal rings are planar, nearly parallel {tilt angles: 1.6° (in **4**), 2.9° and 1.1° (in the two cations of **5**), 1.8° (in **6**), and 1.6° (in **7**)}, and they deviate by ca. 5.8° (in **4**), −1.3° and −3.4° (in **5**), 11.0° (in **6**), or 0.5° (in **7**) from the ideal eclipsed conformation.

In all cases the separation Fe···Pd is greater than the sum of the van der Waals radii of these atoms,[26] thus suggesting that there is no direct interaction between them.

^{57}Fe Mössbauer Studies. In order to clarify if the differences detected in the structures of compounds **4**−**7** affect the electronic environment of the iron(II) center, ^{57}Fe Mössbauer studies were performed. In all cases the spectra consisted of a single quadrupole doublet (Figure 8), thus suggesting a single iron site. The isomer shifts, quadrupole splitting parameters, and line widths are presented in Table 1. It is well known that in ferrocene derivatives the presence of electron-donating groups produces an increase of the quadrupole splitting relative to that of ferrocene, whereas electron-withdrawing substituents have the opposite effect.[27] As shown in Table 1, for the new compounds the quadrupole splitting was smaller than that of ferrocene[28] (ΔE_q = 2.37 mm s^{-1} at room temperature or 2.41 mm s^{-1} at 80 K), thus indicating that the "Pd(η^3-1-R^1-C_3H_4)(-CH=N-CH_2-$(CH_2)_n$-NMe_2" moieties have a stronger electron-withdrawing power than hydrogen in ferrocene. The X-ray crystal structures of **4** and **6** revealed that only one isomer was present in the solid state. In both cases the imine adopted the *anti*-(*E*) conformation and the "Fe(η^5-C_5H_5)" moiety and the C^β of the allyl group were on the same side of the coordination plane of the palladium. Thus, the differences between the ΔE_q values for **4** and **6** indicate that the replacement of the hydrogen in **4** by a phenyl in **6** reduces the electron-withdrawing ability of the substituent bound to the ferrocenyl unit. For the pair of compounds **5** and **7** the variations detected in the ΔE_q parameters do not clearly exceed 3σ, and in these products either two isomers coexist in the solid state (in **5**) or the disorder found in the substituted carbon C^α of the allyl unit does not allow establishing unambiguously the *endo*- or *exo*-conformation of this ligand.

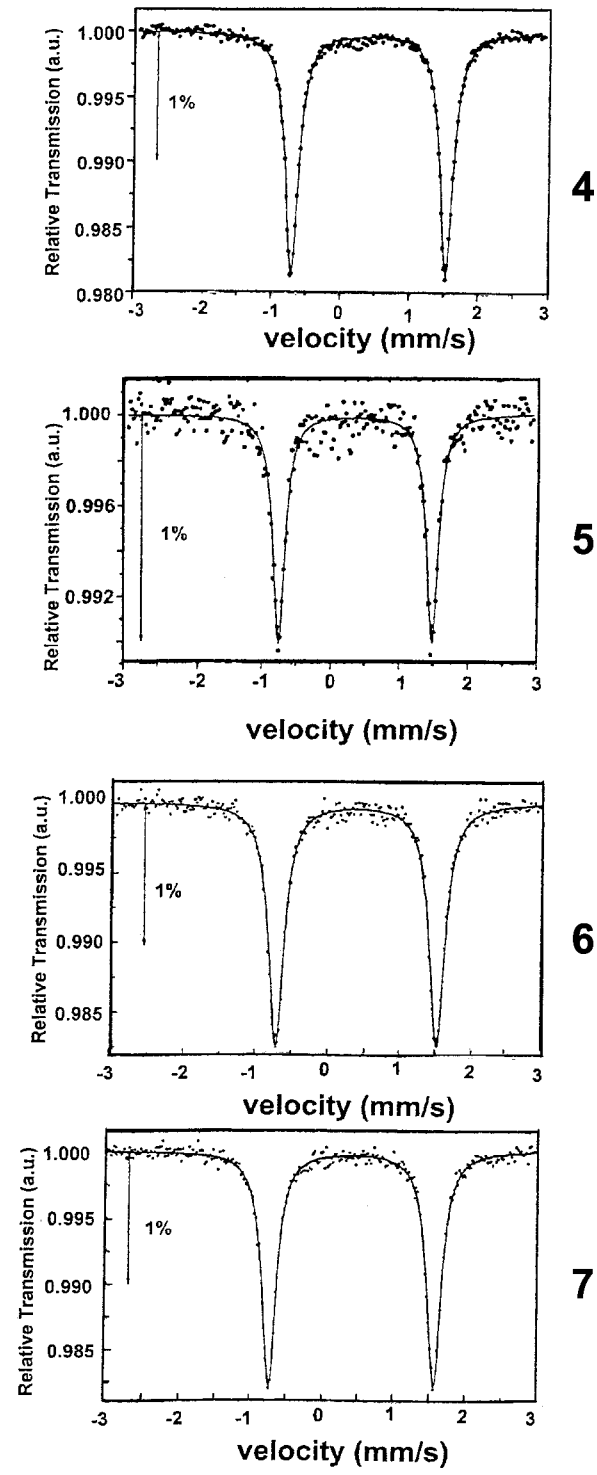

Figure 8. ^{57}Fe-Mössbauer spectra of compounds [Pd(η^3-1-R^1-C_3H_4){FcCH=N-CH_2-$(CH_2)_n$-NMe_2}][PF_6] {R^1 = H and n = 2 (**4**) or 1 (**5**) or R^1 = Ph and n = 2 (**6**) or (**7**)} at 80 K.

Study of the Solution Behavior of Compounds 4−7. One-dimensional and two-dimensional NMR spectra of **4**−**7** have enabled the determination of the number of isomeric species present in solution as well as the structural features of the major

(25) (a) Cravotto, G.; Demartin, F.; Palmisano, G.; Penoni, A.; Radice, T.; Tollari, S. *J. Organomet. Chem.* **2005**, *690*, 2017–2026. (b) Zapt, A.; Beller, M. *Chem. Commun.* **2005**, 431–440. (c) Chen, M.-T.; Huang, C. A.; Chen, C. T. *Eur. J. Inorg. Chem.* **2006**, *464*, 2–4648.

(26) (a) Bondi, A. *J. Phys. Chem.* **1964**, *64*, 441–451. (b) Kitaigorodskii, A. I. *Molecular Crystals and Molecules*; Academic Press: London (UK), 1973.

(27) (a) Houlton, A.; Miller, J. R.; Silver, J.; Jassim, N.; Ahmet, M. J.; Axon, T. L.; Bloor, D.; Cross, G. H. *Inorg. Chim. Acta* **1993**, *205*, 67–70. (b) Houlton, A.; Miller, J. R.; Roberts, R. M. G.; Silver, J. *J. Chem. Soc., Dalton Trans.* **1991**, 467–470.

(28) Houlton, A.; Bishop, P. T.; Roberts, R. M. G.; Silver, J.; Herberhold, M. *J. Organomet. Chem.* **1989**, *363*, 381–389.

components {i.e., the conformation adopted by the ligand and the relative arrangement of the central σ(C−H) bond of the allyl group and the "Fe(η^5-C_5H_5)" unit}.

Proton-NMR spectra of **4** in acetone-d_6 or acetonitrile-d_3 at 298 K showed only one set of resonances, but the signals were broader than expected. Variable-temperature NMR spectra of **4** (in acetone-d_6) at 203 K showed two sets of superimposed signals of relative intensities 10.0:5.5, and the coalescence was achieved at 243 K, thus suggesting the coexistence of two isomeric species in solution that are involved in a fast exchange at room temperature on the NMR time scale. A careful analyses of 2D NMR spectra of **4** allowed us to identify the major component as the *anti*-(*E*), *endo*-isomer (**4$_{\mathbf{I}}$** in Figure 2) and the minor one as the *anti*-(*E*), *exo*-isomer (**4$_{\mathbf{II}}$** in Figure 2). In addition, NMR studies suggested that the energy required for the interconversion of the two isomers **4$_{\mathbf{I}}${***anti*-(*E*), *endo*} and **4$_{\mathbf{II}}${***anti*-(*E*), *exo*} should be relatively small to enable the fast interchange at $T > 243$ K.

^{1}H NMR spectra of **5** at 298 K in acetone-d_6 and in acetonitrile-d_3 showed two sets of superimposed signals (of relative intensities 10.0:3.0 and 10.0:2.4, respectively), indicating the coexistence of two species in solution, which were identified as the {*syn*-(*Z*), *exo*} and {*syn*-(*Z*), *endo*} isomers (Figure 2, **5$_{\mathbf{IV}}$** and **5$_{\mathbf{III}}$**, respectively). Thus, the comparison of the solution behavior of **4** and **5** suggests that the energy required to modify the arrangement of the allyl group (*endo* or *exo*) versus the "Fe(η^5-C_5H_5)" unit in **5** should be higher than that in **4**.

Proton-NMR of **6** in CD_2Cl_2 in the temperature range 223−298 K showed four sets of signals[30] for four isomers. Detailed analysis of the {^{1}H−^{1}H}-NOESY suggests that the major components were the {*anti*-(*E*), *exo, cis*-N_{imine}, *syn*} and the{*anti*-(*E*), *endo, cis*-N_{imine}, *syn*} isomers (Figure 3, **6$_{\mathbf{V'}}$** and **6$_{\mathbf{I'}}$**, respectively). The low abundance of the remaining two species did not allow us to identify unambiguously all the resonances due to the protons of these isomers, but on the basis of the chemical shifts we tentatively postulate that one of them corresponds to the either the {*syn*-(*Z*), *endo, trans*-N_{imine}, *syn*} or to the {*syn*-(*Z*), *exo, trans*-N_{imine}, *anti*} isomer (Figure 3, **6$_{\mathbf{XI'}}$** or **6$_{\mathbf{XVI'}}$**, respectively).

^{1}H NMR spectra of **7** in CD_2Cl_2 in the temperature range 223−298 K suggested the coexistence of three isomers.[31] The analyses of the {^{1}H−^{1}H}-NOESY spectrum of **7** allowed us to identify the major species present in solution as the {*syn*-(*Z*), *exo, cis*-N_{imine}, *syn*} and {*syn*-(*Z*), *exo, trans*-N_{imine}, *syn*} isomers (Figure 3, **7$_{\mathbf{XIII'}}$** and **7$_{\mathbf{XV'}}$**, respectively). The low abundance of the third isomer of **7** precluded the complete identification of this isomer.

As the electrochemical studies of **4**−**7** were conducted in acetonitrile-d_3, CD_2Cl_2 was replaced by CD_3CN, which is more polar and has stronger coordinating ability than CD_2Cl_2, but neither the number of species present in solution nor their relative abundance changed in the NMR studies.[32,33]

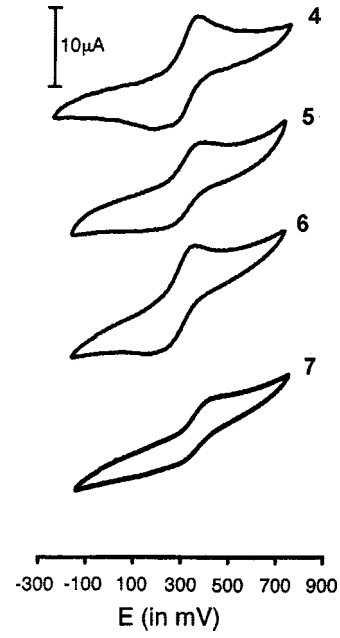

Figure 9. Cyclic voltammograms of compounds [Pd(η^3-1-R^1-C_3H_4){FcCH═N-CH_2-$(CH_2)_n$-NMe_2}][PF_6] {R^1 = H and n = 2 (**4**) or 1 (**5**) or R^1 = Ph and n = 2 (**6**) or (**7**)} in acetonitrile at 298 K and at a scan speed v = 100 mV/s.

Table 2. Electrochemical Data: Anodic and Cathodic Potentials (E_{pa} and E_{pc}, referenced to the ferrocene/ferricinium couple) and Separation between Peaks (ΔE) (in mV) for [Pd(η^3-1-R^1-C_3H_4){FcCH═N-CH_2-$(CH_2)_n$-NMe_2}][PF_6] {R^1 = H and n = 2 (4) or 1 (5) or R^1 = Ph and n = 2(6) or 1(7)} at a Scan Speed v = 100 mV s^{-1}

compound	n	R^1	E_{pa}	E_{pc}	ΔE
4	2	H	358	178	180
5	1	H	381	252[a,b]	[a,b]
6	2	Ph	358	175	183
7	1	Ph	415	278[a,c]	[a,c]

[a] See Figure9. [b] In this case the reduction peak was poorly resolved. [c] The reduction peak was not clearly defined.

Electrochemical Studies. In order to elucidate the effects produced by the coordination of the Schiff bases to the palladium(II) and the nature of the substituent R^1 on the allyl group on the electronic environment of the iron(II), we also carried out electrochemical studies. Electrochemical data for **4**−**7** were obtained from cyclic voltammetric studies of freshly prepared solutions (10^{-3} M) in acetonitrile using (Bu_4N)[PF_6] as supporting electrolyte.

Cyclic voltammograms of **4**−**7** are presented in Figure 9, and the most relevant electrochemical parameters are summarized in Table 2.

As shown in Figure 9 the cyclic voltammograms showed an anodic peak with a directly associated reduction peak in the reverse scan, which in general was less resolved than the anodic one. According to the general rules established for ferrocene derivatives, the presence of electron-withdrawing groups inhibits the oxidation of the iron(II), in contrast with the electron-donor

(29) (a) Drommi, D.; Saporita, M.; Bruno, G.; Fararone, F.; Scafato, P.; Rosini, C. *Dalton Trans.* **2007**, 1509–1519. (b) Pregosin, P. S.; Rüegger, H.; Salzmann, R.; Albinati, A.; Lianza, F.; Kunz, R. W. *Organometallics* **1994**, *13*, 83–90. (c) Pregosin, P. S.; Salzmann, R. *Magn. Reson. Chem.* **1994**, *32*, 128–132. (d) Rüegger, H.; Kunz, R. W.; Ammann, C. J.; Pregosin, P. S. *Magn. Reson. Chem.* **1991**, *29*, 197–203.

(30) The intensity ratio of the signals due to the four isomers of **6** was 10.0:3.1:3.3:0.1 (at 298 K), 10.0:3.4:2.8:0.1 (at 273 K), and 10.0:3.5:2.9:0.1 (at 223 K).

(31) The intensity ratio of the signals due to three the isomers of **7** was 10.0:2.4:0.1 (at 298 K), 10.0:2.1:0.4 (at 273 K), and 10.0:2.3:0.3 (at 223 K).

(32) In acetonitrile-d_3 the four isomers of **6** coexisted in a proportion of 10.0:3.1:2.1:0.1 at 298 K and of 10.0:3.5:2.6:0.1 at 273 K.

(33) In acetonitrile-d_3 the three isomers of **7** coexisted in a relative abundance of 10.0:2.1:0.8 at 298 K and of 10.0:1.9:0.7 at 273 K.

Table 3. Regioselectivities of the Catalytic Allylic Alkylation Reactions Studied at 298 K[a] and Those Reported for Compound 8[b]

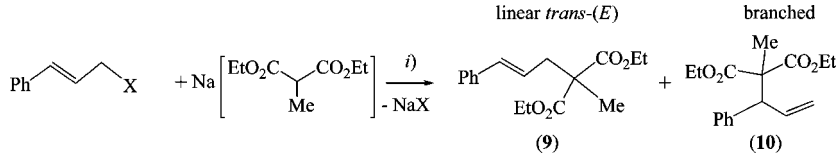

i) Compounds **4**, **5** or **8**.

						final products (%)[c]	
entry	compound	X	solvent	*t* (h)	conversion (%)	**9**	**10**
I	**4**	OAc	THF	3	100.0	98.0	2.0
II	**5**	OAc	THF	3	100.0	97.2	2.8
III	**8**	OAc	THF	3	90.5	94.8	5.2
IV	**8**	OAc	THF	20	100	93.4	6.6
V	**4**	OAc	THF/pentane	3	100.0	97.4	2.6
VI	**4**	OAc	THF/DMF	3	94.3	98.7	1.3
VII	**4**	OAc	THF/DMF	20	100.0	98.6	1.4
VIII	**4**	Cl	THF	3	100.0	98.3	1.7

[a] Experimental conditions: mixtures containing 5×10^{-3} mmol of **4** or **5**, 0.5 mmol of cinnamyl acetate or chloride, 1.0 mmol of sodium diethyl 2-methylmalonate, 5 mL of the corresponding solvent, and decane (0.258 mmol) at 298 K. [b] Data from ref 11. [c] Determined by GC.

Chart 1

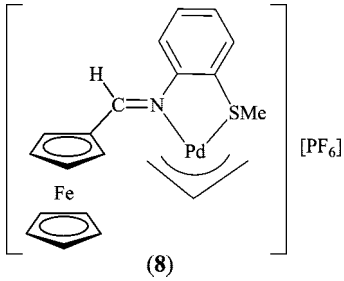

(**8**)

groups, which facilitate the oxidation.[23b,34−36] For compounds under study the position of the anodic peak shifts to higher potentials than for the corresponding ligands {E_{pa} (referred to the ferrocene/ferricinium couple) = 159 and 140 mV for **1** and **2**, respectively},[35] thus indicating that the formation of the six- (in **4** and **6**) or five- (in **5** and **7**) membered chelate ring enhances the electron-withdrawing ability of the substituent on the ferrocenyl unit in comparison with that of the free ligands. This trend is similar to that found for related palladium(II) complexes derived from (N) or (N,E) (E = N′, S)-donor ferrocenyl Schiff bases[11,13b,23b,35,36] and agrees with the conclusions reached from the ^{57}Fe-Mössbauer studies.

Palladium(II)-Catalyzed Allylic Alkylation. Compounds **4** and **5** were tested in the allylic alkylation of cinnamyl acetate using sodium diethyl 2-methylmalonate as nucleophile. The results obtained from these studies are presented in Table 3. For comparison purposes data reported for [Pd(η^3-1-R^1-C_3H_4){FcCH=N-(C_6H_4-2SMe)}][PF_6][11] (**8**) (Chart 1) are also included.

When the catalytic processes were performed in THF under mild experimental conditions (Table 3, entries I and II), the formation of the linear *trans*-(*E*) product (**9**) was strongly preferred over the branched derivative (**10**), and no evidence of the formation of the linear *cis*-(*Z*) isomer was detected by either NMR or gas chromatography (GC). Some authors have demonstrated that for palladium(II) complexes holding bidentate (L,L′) donor ligands an increase of the bite angle of the chelating (L,L′) group favors the formation of larger percentages of the branched derivatives.[5b,37] However, for **4** and **5** {with crystallographic bite angles of 88.6(2)° (in **4**) and 82(2)° (average value for **5**)} the trend (if significant) is just the opposite, thus suggesting that other factors such as electronic and/or steric effects arising from the different conformation of the imine {*anti*-(*E*) in **4** or *syn*-(*Z*) in the two cations present in the crystal structure of **5** (Figure 5)} may be more important in this case as to introduce small variations in the regioselectivity of the process.

The comparison of the results obtained for **4** and **5** (Table 3, entries I and II) and those reported recently for the palladium(II)−allyl compound [Pd(η^3-C_3H_5){FcCH=N-(C_6H_4-2-SMe)}][PF_6][11] (**8**) (entries III and IV) reveals that **4** and **5** are better catalytic percursors than **8**, which contains a bidentate (N,S) ligand. For **4** and **5**, both the conversion and the molar ratio **9**:**10** are higher than for **8** in shorter reaction times.

In a first attempt to clarify if the polarity of the solvent could affect the regioselectivity of the process or its rate, we also studied the catalytic allylic alkylation of cinnamyl acetate using mixtures (1:1) of THF and pentane or dimethylformamide (DMF) (entries V−VII). As can be easily seen in Table 3, a decrease of the polarity of the solvent produces a slight decrease of the relative proportion between the linear *trans*-(*E*) (**9**) and branched (**10**) products. The replacement of pentane by the more polar DMF produces a slight increase of the regioselectivity toward the linear product when compared with the result obtained in THF (we will return to this point later on), but the process is somewhat slower.

Compound **4** was also tested in the allylic alkylation of cinnamyl chloride (Table 3, entry VIII), and the results showed that in this case there is no significant effect of the nature of the leaving group on the activity or on the selectivity of the reaction.

Stoichiometric Allylic Alkylation. We also studied the reactions between compound **6** or **7** with an excess of sodium

(34) (a) Zanello, P.; Cinquantini, A.; Mangani, S.; Opromolla, G.; Pardi, L.; Janiak, C.; Rausch, M. D. *J. Organomet. Chem.* **1994**, *471*, 171–177. (b) Blom, N. F.; Neuse, E. W.; Thomas, H. G. *Trans. Met. Chem.* **1987**, *12*, 301–306. (c) Hoh, G. L. K.; McEwen, W. E.; Kleinberg, J. *J. Am. Chem. Soc.* **1961**, *83*, 3949–3953. (d) Hamamura, K.; Kita, M.; Nonoyama, M.; Fujita, J. *J. Organomet. Chem.* **1993**, *463*, 169–177.

(35) Riera, X.; Caubet, A.; López, C.; Moreno, V. *Polyhedron* **1999**, *18*, 2549–2555.

(36) Bosque, R.; López, C.; Sales, J. *Inorg. Chim. Acta* **1995**, *244*, 141–145.

(37) (a) van Haaren, R. J.; Oevering, H.; Coussens, B. B.; van Strijdonck, G. P. F.; Reek, J. N. H.; Kamer, P. C. J.; van Leeuwen, P. W. N. M. *Eur. J. Inorg. Chem.* **1999**, *123*, 7–1241. (b) van Haaren, R. J.; Druijven; C, J. M.; van Strijdonck, G. P. F.; Oevering, H.; Reek, J. N. H.; Kamer, P. C. J.; van Leeuwen, P. W. N. M *Dalton Trans.* **2000**, *154*, 9–1554.

Table 4. Crystal Data and Details of the Refinement of the Crystal Structures of [Pd(η^3-1-R^1-C_3H_4){FcCH=N-CH_2-$(CH_2)_n$-NMe_2}][PF_6] {R^1 = H and n = 2 (4) or 1 (5) or R^1 = Ph and n = 2 (6) or 1 (7)} (standard deviation parameters are given in parentheses)

	4	5	6	7
empirical formula	$C_{19}H_{27}F_6FeN_2PPd$	$C_{18}H_{25}F_6N_2FePdP$	$C_{25}H_{31}F_6FeN_2PPd$	$C_{24}H_{29}F_6FeN_2PPd$
fw	590.65	576.62	666.74	652.71
T (K)	293(2)	293(2)	293(2)	293(2)
λ (Å)	0.71069	0.71069	0.71069	0.71069
cryst size (mm × mm × mm)	0.1 × 0.1 × 0.2	0.1 × 0.1 × 0.2	0.1 × 0.1 × 0.2	0.1 × 0.1 × 0.2
cryst syst	orthorhombic	monoclinic	orthorhombic	orthorhombic
space group	$P2_12_12_1$	$P2_1/c$	$P2_1cn$	$Pcab$
a (Å)	9.717(1)	16.188(1)	11.248(10)	16.990(1)
b (Å)	14.296(1)	12.580(1)	12.039(6)	17.240(1)
c (Å)	16.165(1)	21.091(1)	19.803(4)	17.647(1)
α (deg)	90.0	90.0	90.0	90.0
β (deg)	90.0	92.701(1)	90.00	90.0
γ (deg)	90.0	90.0	90.0	90.0
V (Å^3)	2245.5(3)	4290.3(5)	2682(3)	5168.9(5)
Z	4	8	4	8
D_{calcd} (Mg × m^{-3})	1.747	1.785	1.651	1.677
μ (mm^{-1})	1.575	1.647	1.330	1.378
F(000)	1184	2304	1344	2624
θ range for data collection (deg)	2.10 to 31.61	1.26 to 31.52	2.06 to 30.00	2.04 to 31.63
no. of collected reflns	15 115	14 780	7718	58 227
no. of unique reflns [R_{int}]	3223 [0.0330]	6317 [0.0285]	7718 [0.0000]	8585 [0.0359]
no of params	318	577	325	413
goodness of fit on F^2	1.140	1.096	0.998	1.230
R indices {$I > 2\sigma(I)$}	R_1 = 0.0464, wR_2 = 0.1359	R_1 = 0.0466, wR_2 = 0.1210	R_1 = 0.0547, wR_2 = 0.1097	R_1 = 0.0647, wR_2 = 0.1716
R indices (all data)	R_1 = 0.0545, wR_2 = 0.1538	R_1 = 0.0485, wR_2 = 0.1224	R_1 = 0.1097, wR_2 = 0.1351	R_1 = 0.0691, wR_2 = 0.1816
abs struct param	0.019(4)		0.02(3)	

diethyl 2-methylmalonate in THF at 298K (stoichiometric reaction). These reactions were instantaneous and gave after workup a mixture of the *trans*-(*E*) isomer of the linear product (**9**) and the branched derivative (**10**) in molar ratios of 99.92:0.08 (for **6**) and 99.98:0.02 (for **7**). As already observed in catalytic experiments, the *cis*-(*Z*) isomer of the linear product was not detected.

The studies described in the preceding section have shown that for **6** the two major species present in solution correspond to the isomers {*anti*-(*E*), *exo, cis*-N_{imine}, *syn*} and {*anti-(E), endo, cis*-N_{imine}, *syn*} ($\mathbf{6_{V'}}$ and $\mathbf{6_{I'}}$ in Figure 3), and for **7** the major component is the {*syn*-(*Z*), *exo, cis*-N_{imine}, *syn*} isomer ($\mathbf{7_{XIII'}}$ in Figure 3). In the three cases the attack of the nucleophile to the nonsubstituted terminal carbon (C^{γ}) of the allyl unit would yield the *trans*-(*E*) isomer of the linear product (**9**). Consequently, the regioselectivity found for the stoichiometric reactions indicates that the nucleophilic attack takes place *trans* to the imine nitrogen. It should be noted that the regioselectivity of the stoichiometric reactions was higher than those obtained in the catalytic processes (Table 3). The rates of (a) the isomerization process between the different species present in solution or (b) the nucleophilic attack to these isomers might be two of the factors that may influence the small differences detected in the regioselectivities of the stoichiometric and catalytic processes under study. Several authors have also detected variations of the regioselectivity of the catalytic and the stoichiometric alkylation process.[37]

Theoretical Studies. In a first attempt to explain the differences detected in the crystal structures of **4** and **5** we decided to undertake DFT calculations for the four isomers of the cations of **4** and **5** (Figure 2, types I−IV). The theoretical calculations were performed at the B3LYP computational level[38] with the Gaussian03 package[39] using the LANL2DZ basis set.[40] For the cations $\mathbf{4_I}$, $\mathbf{5_{III}}$, and $\mathbf{5_{IV}}$, the values of bond lengths and angles obtained for the optimized geometries were in good agreement with those obtained from X-ray diffraction studies of **4** and **5** described above.

The results showed that the cation $\mathbf{4_I}$ {*anti*-(*E*), *endo*} is the most stable isomer for this compound, which is the same as that found in the crystal structure of **4**, and also the major isomer observed in solution (*vide supra*). Besides that, the differences between the calculated total energies (ΔE, in kcal/mol) for the remaining isomers of **4** and that obtained for $\mathbf{4_I}$ were $\Delta E = 8.3 \times 10^{-2}$ (for $\mathbf{4_{II}}$), 3.12 (for $\mathbf{4_{III}}$), and 3.2 kcal/mol (for $\mathbf{4_{IV}}$). According to these data, the isomers of **4** containing the ligand in the *anti*-(*E*) form ($\mathbf{4_I}$ and $\mathbf{4_{II}}$) are more stable than $\mathbf{4_{III}}$ and $\mathbf{4_{IV}}$, in which conformation of the Schiff base is *syn*-(*Z*). In addition, the low value of ΔE obtained for $\mathbf{4_{II}}$ suggests that the energy required for the conversion $\mathbf{4_I} \rightarrow \mathbf{4_{II}}$, which involves the *endo* → *exo* isomerization of the allyl group, is small. The results obtained from VT-NMR studies indicated that the

(38) (a) Becke, A. D. *J. Chem. Phys.* **1993**, *98*, 5648–5652. (b) Lee, C.; Yang, W.; Parr, R. G. *Phys. Rev. B* **1988**, *37*, 785–789.

(39) Frisch, M. J.; Trucks, G. W.; Schlegel, H. B.; Scuseria, G. E.; Robb, M. A.; Cheeseman, J. R.; Montgomery, J. A., Jr.; Vreven, T.; Kudin, K. N.; Burant, J. C.; Millam, J. M.; Iyengar, S. S.; Tomasi, J.; Barone, V.; Mennucci, B.; Cossi, M.; Scalmani, G.; Rega, N.; Petersson, G. A.; Nakatsuji, H.; Hada, M.; Ehara, M.; Toyota, K.; Fukuda, R.; Hasegawa, J.; Ishida, M.; Nakajima, T.; Honda, Y.; Kitao, O.; Nakai, H.; Klene, M.; Li, X.; Knox, J. E.; Hratchian, H. P.; Cross, J. B.; Bakken, V.; Adamo, C.; Jaramillo, J.; Gomperts, R.; Stratmann, R. E.; Yazyev, O.; Austin, A. J.; Cammi, R.; Pomelli, C.; Ochterski, J. W.; Ayala, P. Y.; Morokuma, K.; Voth, G. A.; Salvador, P.; Dannenberg, J. J.; Zakrzewski, V. G.; Dapprich, S.; Daniels, A. D.; Strain, M. C.; Farkas, O.; Malick, D. K.; Rabuck, A. D.; Raghavachari, K.; Foresman, J. B.; Ortiz, J. V.; Cui, Q.; Baboul, A. G.; Clifford, S.; Cioslowski, J.; Stefanov, B. B.; Liu, G.; Liashenko, A.; Piskorz, P.; Komaromi, I.; Martin, R. L.; Fox, D. J.; Keith, T.; Al-Laham, M. A.; Peng, C. Y.; Nanayakkara, A.; Challacombe, M.; Gill, P. M. W.; Johnson, B.; Chen, W.; Wong, M. W.; Gonzalez, C.; Pople, J. A. *Gaussian 03, Revision C.02*; Gaussian, Inc.: Wallingford, CT, 2004.

(40) (a) Hay, P. J.; Wadt, W. R. *J. Chem. Phys.* **1985**, *82*, 270–283. (b) Wadt, W. R.; Hay, P. J. *J. Chem. Phys.* **1985**, *82*, 284–298. (c) Hay, P. J.; Wadt, W. R. *J. Chem. Phys.* **1985**, *82*, 299–310.

interconversion takes place at room temperature and, consequently, the energy of the isomerization process is expected to be low.

For compound **5**, the {*syn*-(*Z*), *endo*} isomer (**5III**) is more stable than **5IV** {*syn*-(*Z*), *exo*} and the ΔE (0.27 kcal/mol) is greater than the difference obtained for **4I** and **4II** (8.3×10^{-2} kcal/mol), but its magnitude is relatively small. Thus, the similarity of the molar ratios between the two isomeric species of **5** present in solution (in the range of temperatures studied) suggests that the energy of the barrier for the *endo* → *exo* isomerization should be high enough as to hinder the process at room temperature.

On the other hand, the results obtained from the theoretical studies indicate that from an energetic point of view, the changes of the conformation of the Schiff base {*anti*-(*E*) ⇄ *syn*-(*Z*)} are unlikely to occur in both cases.[41]

In addition, the theoretical studies indicated that in the optimized geometries of isomers **5III** and **5IV** one of the hydrogen atoms of the ═N-CH_2- unit is close to one of the protons of the C_5H_4 ring {distances: H(9A)−H(12) = 2.145 and 2.11 Å in **5III** and **5IV**, respectively}. The separation between these groups is similar to that found in the crystal structure {H(9A)−H(12A) = 2.18 Å and H(9B)−H(12B) = 2.09 Å}. Thus, the relative arrangement of these fragments may hinder the *syn* ⇄ *anti* isomerization of the ligand in these isomers.

Additionally, the comparison of the Mulliken charges (*q*) of the terminal carbon atoms of the allyl ligand in the major isomers of **4** present in solution (**4I** and **4II** depicted in Figure 2) shows that the electrophilicity of the carbon atom in a *cis*-arrangement to the imine nitrogen is slightly higher than that of the carbon at the other end of the allyl group.[42] In contrast with these results, for the C^{α} and C^{γ} atoms of **5III** and **5IV** (Figure 2) the *q*-values follow the opposite trend.[43] These findings suggest that from an electronic point of view, the conformation of the ligand in the allyl complexes may introduce tiny variations in the proclivity of the two terminal carbon atoms of the allyl group to undergo the attack of the nucleophile.

Conclusions

The studies presented in this work have provided evidence of the effect induced by the length of the "−$(CH_2)_n$−" backbone of ligands **1** or **2** in the structures and the solution behavior of their palladium(II) allyl complexes **4**−**7**. This affects (a) the conformation of the ligand in the solid state *anti*-(*E*) (in **4** and **6**, which contain a six-membered ring) or *syn*-(*Z*) (in **5** and **7** with a five-membered chelate) and (b) the relative arrangement between the phenyl group and the imine nitrogen {*trans* (in **6**) or *cis* (in **7**)}. The catalytic studies as well as the results obtained from the stoichiometric reactions revealed that, concerning regioselectivity, the formation of the linear product (**9**) is strongly preferred over the branched derivative (**10**), and in both systems there is a complete selectivity for the *trans*-isomer of **9**. These findings indicate that in all cases the nucleophile attacks on the nonsubstituted carbon of the (η^3-1-Ph-C_3H_4) group in the intermediate species formed during the catalytic allylic alkylation of cinnamyl acetate or chloride. The comparison of the results obtained from the catalytic studies performed using **4** or **5** with a bidentate (N,N′) ligand and those reported for **8**, where the Schiff base behaves as a (N,S) group, provided conclusive evidence of the relevancy of the nature of the terminal donor atom N′ (in **4** and **5**) or S (in **8**) of the bidentate ligands in the catalytic activity of the palladium(II) allyl complexes.

(41) The ΔE value for **4III** and **4I** is 3.12 and that between **4IV** and **4II** is 3.23 kcal/mol.

(42) Mulliken charges of the carbon of the allyl group in a *cis*-arrangement to the imine nitrogen are −0.214 (in **4I**) and −0.216 (in **4II**) and for the carbon at the other end, −0.223 (in **4I**) and −0.219 (in **4II**).

(43) For **5III** and **5IV** the Mulliken charges are −0.236 and −0.235, respectively, for the carbon atoms in a *cis*-arrangement to the imine nitrogen and −0.231 and −0.230 for the carbon atom in a *trans*-disposition.

Experimental Section

General Comments. The ligands [FcCH═N-CH_2-$(CH_2)_n$-NMe_2] {with n = 2 (**1**) or 1 (**2**)} and [Pd(η^3-1-R^1-C_3H_4)(μ-Cl)]$_2$ (with R^1 = H or Ph) were prepared as described previously,[12,13b,14] and K[PF_6] was obtained from commercial sources and used as received. Sodium diethyl-2-methylmalonate (0.5 or 0.7 M in THF) was prepared from diethyl 2-methylmalonate and NaH in THF at 273 K. The solvents used were dried and distilled according to the procedures described previously.[44] Elemental analyses (C, H, and N) were carried out at the Serveis de Recursos Cientifics i Tècnics (Universitat Rovira i Virgili, Tarragona). Infrared spectra were obtained with a Nicolet-400FTIR instrument using KBr pellets. FAB^+ mass spectra were registered at the Servei d′ Espectrometria de Masses (Universitat de Barcelona) with a VG-Quattro instrument using 4-nitrobenzyl alcohol (NBA) as matrix. Routine ^{1}H NMR spectra were recorded at ca. 298 K on a Gemini-200 MHz. High-resolution ^{1}H NMR experiments, two-dimensional spectra [{^{1}H−^{1}H}-NOESY and {^{1}H−^{13}C} heteronuclear correlation experiments (HSQC and HMBC)] and variable-temperature NMR experiments were recorded with either a Varian VRX-500 or a Bruker Avance DMX-500 instrument. ^{13}C{^{1}H} NMR spectra were obtained with a Mercury-400 instrument. The solvents used for all the NMR studies are specified in the characterization section of each complex. In all cases the chemical shifts (δ) are given in ppm and the coupling constants (J) in Hz.

Preparation of the Compounds. [Pd(η^3-C_3H_5){FcCH═N-CH_2-$(CH_2)_n$-NMe_2}][PF_6] {with n = 2 (4) or 1 (5)}. A solution formed by the corresponding ligand [FcCH═N-CH_2-$(CH_2)_n$-NMe_2] {n = 2 (**1**) or 1 (**2**)} (8.20×10^{-4} mol),[12,13b] [Pd(η^3-C_3H_5)(μ-Cl)]$_2$ (0.150 g, 4.10×10^{-4} mol),[14a] K[PF_6] (0.180 g, 1.02×10^{-3} mol), and 20 mL of acetone was stirred at room temperature (∼293 K) for 2.5 h. After this period the undissolved materials were removed by filtration and the filtrate was concentrated to dryness on a rotary evaporator. The deep-orange residue was dissolved in a minimum amount of CH_2Cl_2 (distilled and dried) and filtered out. Concentration to dryness of the filtrate under reduced preasure gave an orange solid, which was collected, air-dried, and then dried under vacuum for two days {yields: 0.290 g (60%) and 0.212 g (45.0%) for **4** and **5**, respectively}. The complexes were recrystallized in a 1:1 mixture of CH_2Cl_2 and *n*-hexane. The quality of the crystals of **5** was poor, but attempts to obtain better crystals of this product were unsuccesful.

[Pd(η^3-1-Ph-C_3H_4){FcCH═N-CH_2-$(CH_2)_n$-NMe_2}][PF_6] {with n = 2 (6) or 1 (7)}. These products were prepared according to the procedure described for **4** and **5**, but using the corresponding amount of [Pd(η^3-1-Ph-C_3H_4)(μ-Cl)]$_2$.[14b] In these cases the isolated solids were recrystallized in a CH_2Cl_2/Et_2O (1:1) mixture {yields: 0.417 g, (65.0%) and 0.319 g (55%) for **6** and **7**, respectively}.

Typical Procedure for Allylic Alkylation. The catalytic reactions were performed at room temperature (298 K) in THF (5 mL) using 1% of the catalyst (**4** or **5**) (5×10^{-6} mol), 5×10^{-4} mol of cinnamyl acetate or chloride, and 1×10^{-3} mol of sodium diethyl 2-methylmalonate. The progress of the reaction was monitored by taking samples of the reaction mixture at different time intervals (before the addition of the nucleophile and after 3, 20, and 40 h),

(44) Armarego, W. L. F.; Perrin, D. D. *Purification of Laboratory Chemicals*, 4th ed.; Butterworth-Heinemann: Oxford (UK), 1996.

which were later on diluted with Et_2O, washed with water, dried over $MgSO_4$, and analyzed by gas chromatography using decane as internal standard. The stoichiometric alkylation reactions were carried out at 298 K by adding an excess of sodium diethyl 2-methylmalonate (0.8 mL of a 0.7 M solution in THF) to a solution containing 80 mg (1.20×10^{-4} mol) of **6** {or 80 mg, 1.23×10^{-4} mol) of **7**} in 8 mL of THF. After 10 min, the reaction mixture was poured into 10 mL of H_2O, filtered over Celite, and extracted with Et_2O, and the combined fractions were dried over $MgSO_4$. The evaporation of the solvent gave an oily residue, which was disolved in a minimum amount of Et_2O and passed through a SiO_2 chromatography column (4.0 cm × 0.6 cm) using Et_2O as eluant. The band was collected and concentrated to dryness on a rotary evaporator, giving the alkylation products.

The product distribution was determined by ^{1}H NMR (500 MHz) and with gas chromatography (Trace DSQ equipped with a HP-5 column, 25 m in length, inner diameter of 0.2 mm, and film thickness of 0.5 μm).

^{57}Fe-Mössbauer Studies. Mössbauer spectra were recorded using powdered solid samples. The samples were placed in liquid N_2, quenched to 80 K, and transferred to an Oxford Instruments cryostat. Spectra were collected at 80 K using a constant acceleration Mössbauer spectrometer with a ^{57}Co/Rh source. The source was moved via triangular velocity wave, and the γ-counts were collected in a 512 multichannel analyzer. Velocity calibration was done using a 25 μm thick metallic iron foil, and the Mössbauer spectral parameters (presented in Table 1) are given to this standard at room temperature.

Electrochemical Studies. Electrochemical data for compounds under study were obtained by cyclic voltammetry under nitrogen at 298 K using acetonitrile (HPLC grade) as solvent and tetrabuthylammonium hexafluorophosphate {$(Bu_4N)[PF_6]$, 0.1 M} as supporting electrolyte and a M263A potentiostat from EG&G instruments. The potentials were referenced to an Ag-$AgNO_3$ (0.1 M in acetonitrile) electrode separated from the solution by a medium-porosity fritted disk. A platinum wire auxiliary electrode was used in conjunction with a platinum disk working Tacussel-EDI rotatory electrode (3.14 mm^2). Cyclic voltammograms of ferrocene were recorded before and after each sample to ensure the stability of the Ag-$AgNO_3$ electrode. Cyclic voltammograms of freshly prepared solutions (10^{-3} M) of the samples in acetonitrile were run, and the values of measured potentials were then referred to ferrocene, which was used as internal reference. Under these experimental conditions the standard error of the measured potentials was ±5 mV. In all experiments, cyclic voltammograms were registered using scan speeds varying from 10 to 100 mV s^{-1}.

Crystallography. A prismatic crystal of **4**, **5**, **6**, or **7** (sizes in Table 4) was selected and mounted on a MAR345 diffractometer. Unit cell parameters were determined from automatic centring of 13 504 (for **4**), 10 542 (for **5**), 38 174 (for **6**), and 38 174 (for **7**) reflections in the range $3° < \theta < 31°$ and refined by the least-squares method. Intensities were collected with graphite-monochromatized Mo Kα radiation. The number of reflections collected was 15 115 (in the range $2.10° < \theta < 31.6°$, for **4**), 14 780 ($2.26° < \theta < 31.52°$, for **5**), 7718 ($2.06° < \theta < 30.00°$, for **6**), and 58 227 ($2.05° < \theta < 31.6°$, for **7**), of which 3223 (for **4**), 6267 (for **5**), 7718 (for **6**), and 8535 (for **7**) reflections were nonequivalent by symmetry. For **5** Lorentz−polarization corrections and absorption corrections were made, while in the remaining cases only Lorentz−polarization corrections were done.

The structures were solved using direct methods, using the SHELXS computer program,[45] and refined by full-matrix least-squares method with the SHELX97 computer program.[46] The function minimized was $\sum w||F_o|^2 - |F_c|^2|^2$, where $w = [\sigma^2(I) + (0.0966P)^2 + 2.0199P]^{-1}$ (for **4**), $w = [\sigma^2(I) + (0.0.526P)^2 + 13.0102P]^{-1}$ (for **5**), $w = [\sigma^2(I) + (0.0637P)^2]^{-1}$ (for **6**), and $w = [\sigma^2(I) + (0.0784P)^2 + 4.072P]^{-1}$ (for **7**), and $P = (|F_o|^2 + 2|F_c|^2)/3$; f, f', and f" were obtained from the literature.[47] For **4** and **6** the crystals were twinned and the final Flack coefficients[48] were 0.019(4) (for **4**) and 0.02(3) (for **6**). Further details concerning the resolution and refinement of these crystal structures are presented in Table 4.

Theoretical Studies. Calculations were carried out at the B3LYP computational level[38] with the Gaussian03 package[39] using LANL2DZ basis set.[40] Geometry optimizations were performed without any geometry restriction.

Supporting Information Available: Characterization data {elemental analyses and MS, IR, and NMR spectroscopic data} and full details of the crystallographic analyses of **4**−**7** in CIF format. This material is available free of charge via the Internet at http://pubs.acs.org.

Acknowledgment. This work was supported by the Ministerio de Ciencia y Tecnología of Spain (Grant BQU2003-00906) and FEDER funds.

OM7012452

(45) Sheldrick, G. M. *SHELXS, A computer program for determination of crystal structures*; University of Göttingen: Germany, 1997.
(46) Sheldrick, G. M. *SHELXL-97, A computer program for determination of crystal structures*; University of of Göttingen: Germany, 1997.
(47) *International Tables of X-Ray Crystallography*; Kynoch Press: Birmingham (UK), 1979; Vol. IV, pp 99, 100, and 149.
(48) Flack, H. D. *Acta Crystallogr.* **1983**, *A39*, 867–881.